PHYSICAL REVIEW A VOLUME 22, NUMBER 3 SEPTEMBER 1980

Wavelengths and fine structure of $2s$-$2p$ transitions in two- and three-electron ions

H. G. Berry, R. DeSerio,* and A. E. Livingston†
Argonne National Laboratory, Argonne, Illinois 60439
(Received 12 December 1979)

We present an analysis of our recent experimental wavelengths for the $1s2s\,^3S_1$-$1s2p\,^3P_{0,2}$ transitions of Cl XVI and compare the results with theory and other experiments for the He I isoelectronic sequence. The limits of precision of wavelength measurements obtained using fast-ion-beam sources are detailed. We discuss the limited precision of present theory for the energies of bound states of the relativistic two-electron systems and show that higher-order quantum electrodynamic and relativistic corrections are needed to obtain agreement with our measurements. We present a similar comparison of experiment and theory for the resonance transitions $2s\,^2S$-$2p\,^2P$, of the Li I isoelectronic sequence and discuss recent results for systems of more electrons. We conclude that many useful tests of multielectron quantum electrodynamic and relativistic corrections can be made by existing and future measurements of wavelengths and fine structure in medium-Z ions of a few electrons.

I. INTRODUCTION

We have recently published[1] an initial set of results for the two transition wavelengths $1s2s\,^3S_1$-$1s2p\,^3P_2$ and $1s2s\,^3S_1$-$1s2p\,^3P_0$ in two-electron Cl XVI. In this paper we present a more detailed description of the data analysis involved in obtaining the precision claimed, and of the present state of atomic theory for two-electron atoms. We extend our theoretical analysis of the two-electron system by comparing a similar analysis for three-electron atoms with the experimental wavelengths of the resonance transitions $1s^2 2s\,^2S_{1/2}$-$1s^2 2p\,^2P_{1/2,3/2}$.

We discuss the feasibility and problems of using such wavelength measurements as tests of quantum electrodynamics (QED). For lower-Z ions, we have previously summarized[2,3] experimental measurements for two-electron ions of $Z \leq 10$. The experimental accuracy attained for the QED shifts in such ions is generally an order of magnitude less than that for one-electron ions. In addition, the theoretical precision for the Lamb shift is limited by the calculation of two-electron correlation effects.[4] Ermolaev[4] verified that for Li^+ these effects could account for the differences between the observed and the hydrogenic-Lamb-shift values in the $1s2s$ and $1s2p$ states. However, as also pointed out by Kastner,[5] for higher-Z ions, measurements of the $\Delta n = 0$ transition energies can lead to more sensitive testing of quantum electrodynamic and relativistic corrections. The nonrelativistic part becomes a smaller fraction of the transition energy as the ion becomes more hydrogenic and degenerate in character, while electron correlation parts will also be reduced for the QED and relativistic contribution corrections. Davis and Marrus[6] made the first $2s\,^3S$-$2p\,^3P$ observation for heliumlike ions of $Z > 10$ in their measurement of Ar XVII. Within their limited precision of ±1 Å, the results were in agreement with theory.[7] Our greatly improved precision in the wavelength measurement of the same transition in Cl XVI[1] is sufficient to test one-electron QED theory at the few parts per thousand level, provided that all two-electron relativistic and nonrelativistic effects can be calculated to the same absolute precision. We show in the paper that such effects can be calculated to about this same precision for $2s\,^3S_1$-$2p\,^3P_2$ transition for nuclei of charge Z in the range of 15 and higher. Thus, at present, these measurements provide tests both of high-order relativistic and QED corrections to atomic energies. They point out the need for a consistent nonperturbative treatment of relativistic atoms with more than one electron. One purpose of our work is to show that having accounted correctly for the two- and many-electron effects, such measurements provide more accurate tests of one-electron QED effects than presently possible by direct measurements in one-electron atoms.[8] Since our first Cl XVI measurement,[1] one other measurement of less precision has been made in two-electron silicon.[9]

II. EXPERIMENT

Most of the details of our beam-foil measurement of the $2s\,^3S_1$-$2p\,^3P_{0,2}$ transitions of Cl XVI are given in Ref. 1. A 1-m normal incidence concave grating monochromator (McPherson model 225) was used to view the beam at about 90° to the beam axis in the standard beam-foil geometry. The monochromator was refocused[10] by adjustment of the grating position and entrance slit to provide optimum resolution for an 80-MeV chlorine beam

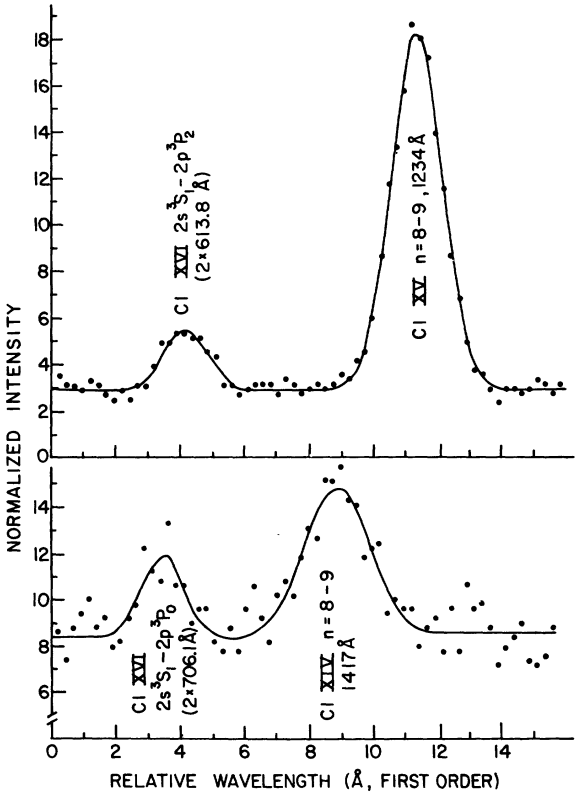

FIG. 1. Wavelength scans including the Cl XVI $2s^3S_1$-$2p^3P_2$ transition near 2×614 Å (upper) and the Cl XVI $2s^3S_1$-$2p^3P_0$ transition near 2×706 Å (lower). The solid line represents a fit using Gaussian profiles.

(beam velocity $\beta = v/c = 0.070$). This provided an important reduction in linewidth from a half-width of about 9 Å for a nonrefocused monochromator. Our linewidth was determined by the large slit-widths required on account of the weak source intensity. Slit widths of 150 μm were used for most of the spectra which gave linewidths of about 1.5 Å in first order (0.75 Å in second order for our line of interest).

The monochromator wavelength drive was coupled to a stepping motor controlled by pulses from an on-line PDP 11/45 computer. The spectra were collected by integrating a constant beam charge from a Faraday cup at each wavelength position. At the end of each spectral scan we checked the background count before repeating the same spectral range. Individual spectra were summed after dark count subtraction and Fig. 1 shows a sum of six individual scans. All spectra were recorded in terms of a known number of stepping motor pulses from the zero-order position of the monochromator. Thus, relative wavelengths could be determined for all chlorine spectral lines observed in the range 300 to 1800 Å.

III. ANALYSIS OF THE DATA

The reduction of the observed spectra to precision wavelengths for the two heliumlike chlorine transitions $2s\,^3S_1 \rightarrow 2p\,^3P_2$ and $2s\,^3S_1 \rightarrow 2p\,^3P_0$ consists of two principal parts: The establishment of accurately known calibration wavelengths and the measurement of the wavelength separations from the transitions of interest to these calibration wavelengths. We analyze these two aspects separately below.

A. Calibration lines

It has long been known that the beam-foil light source produces strong populations in high (n, l) states giving rise to strong yrast transitions of the type $(n, l=n-1) \rightarrow (n-1, l=n-2)$. In the first beam-foil spectra of high-energy ion beams[11] it was noted that such transitions dominate the spectra. The fine structure of the different l states is rarely resolved, the transitions being closely hydrogenlike for the nonpenetrating orbits. Hence, these transition wavelengths are easily calculated and become natural calibration lines in beam-foil spectra, as suggested previously.[12,13]

At the beam energies used, we see yrast transitions from chlorine ions of 2–5 electrons, and several of these are shown in Fig. 2. The energy levels contributing to these transitions have generally been described in terms of a relativistic hydrogenic part plus a core polarization part.[14] In particular, for nonpenetrating orbits of high

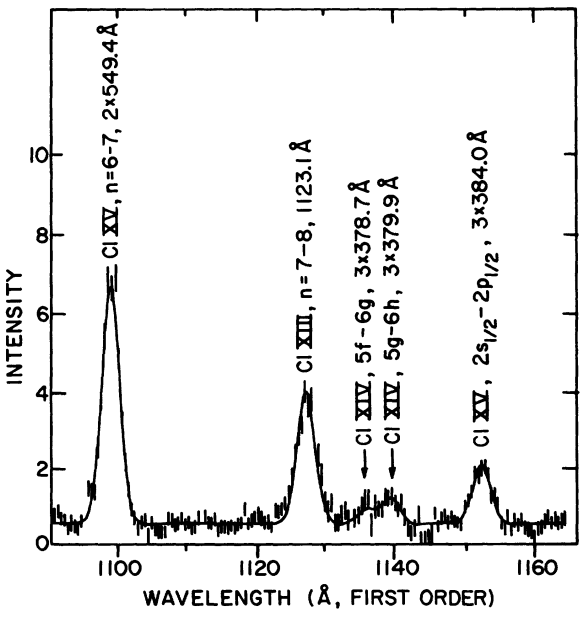

FIG. 2. A survey wavelength scan of the spectrum from foil excited chlorine at 80-MeV beam energy.

angular momentum, the hydrogenic term value $T_H(n, l)$ is the dominant part of the total term value $T(n, l)$ where

$$T(n, l) = T_H(n, l) + \Delta_p(n, l), \quad (1)$$

and $\Delta_p(n, l)$ represents the polarizability of the core inside the valence electron. The polarization term has been expanded in the nonrelativistic limit in terms of the multipole moments of the core

$$\Delta_p(n, l) = A(Z)P(n, l)[1 + k(Z)q(n, l) + \cdots], \quad (2)$$

where $P(n, l)$ and $q(n, l)$ are functions[14] of the principal quantum number n and orbital quantum number l, A is proportional to the dipole moment, Ak is proportional to the quadrupole moment, etc., of the core. For high-Z ions, and for precision wavelengths, relativistic corrections to A and k are needed. Alternatively, Eq. (2) can be treated as a phenomenological fit to the wavelengths of a particular ion and A, k become effective dipole and quadrupole moments of the core. Very few measurements of such effective multipole moments have been made where relativistic effects become important. Measurements in light ions and some measurements in higher-Z alkalilike ions show good agreement with Eq. (2) which can then be used to estimate ionization potentials.[14]

Several calculations of the multipole moments of ionic cores of a few electrons have been made.[15] For two-electron ions, the one-electron core polarizability is known exactly in the nonrelativistic limit.[15]

In the three-electron ions, the core of $1s^2$ is tightly bound with a very small polarizability, and the dipole polarizability can be written[16,17]

$$A(Z) = 9\zeta^4(Z - s)^{-4}, \quad (3)$$

for an ionization stage ζ (the net charge seen by the outer electron), and a screening constant s given by[14]

$$s = 0.3417 + 0.098(Z - s)^{-1}. \quad (4)$$

Thus, for chlorine, $s = 0.3476$ and $A = 5.925$ cm^{-1}. The quadrupole polarizability is then

$$k/\sqrt{A} = 0.263\zeta + 0.577 - 0.82/(\zeta + 1), \quad (5)$$

giving for chlorine $k = 10.88$ cm^{-1}.

We use the three-electron Cl XV $n = 8$-9 transition as a calibration line. From Eqs. (3)–(5) we find the polarizability corrections $\Delta_p(n, l)$ are less than 1 cm^{-1} for $l > 3$ for the $n = 8$ and 9 levels. Edlén[14] has derived slightly different polarization parameters for the Li I isoelectronic sequence (for Cl XVI, he finds $A = 5.9227$ cm^{-1} and $k = 9.8537$). Both his values and the expansions given above give excellent agreement with experiment for $Z \leq 9$ and for $Z = 13$ and 14 (Ref. 18). The relativistic hydrogenic energies with core charge $\zeta = 15$ then provide wavelengths to better than this accuracy. It should, however, be noted that the Dirac-fine-structure splittings have only been tested to high accuracy in low $n(\leq 4)$ in hydrogen and helium.

The Cl XVI $n = 8$-9 transition, used as a calibration line for the $^3S_1$-$^3P_0$ line, has significant polarization shifts since the $1s^2 2s$ core is not tightly bound. As is shown in Fig. 2, we resolved the $5g$-$6h$ and $5f$-$6g$ transitions of Cl XIV. In our initial paper[1] we used this fine-structure separation of 1065 ± 250 cm^{-1} to deduce a dipole constant [Eq. (2)] for the core of $A = 645 \pm 160$ cm^{-1}, and then determine the fine structure of the Cl XIV $n = 8$-9 transition. However, it has been pointed out by Curtis,[19] that theoretical values of the dipole and quadrupole polarizabilities can be obtained for the whole isoelectronic sequence; but further, these theoretical values do not agree with observed measurements of the nf and ng levels in other less ionized atoms in the beryllium sequence.[20] This is due to configuration mixing with the displaced term system, and in Cl XIV, the $2s6l$ levels are perturbed by the nearby $2p5l'$ levels. The $n = 8$-9 transition of Cl XIV is not expected to be as perturbed by displaced term system members. There are no displaced terms near the $2s9l$ levels while the $2p6l'$ levels lie below the $2s8l$ levels, and will perturb mainly the lower-L values which do not contribute strongly to the $n = 8$-9 transition. The predicted polarizability[19] for Cl XIV is $A = 2500$ cm^{-1} and we have used this number to obtain calculated wavelengths for the $n = 8$-9 transitions. These are considerably different from our previous estimates based on the $n = 5$-6 fine structure. Apart from the displaced term mixing, the isoelectronic expansion of the polarizability parameters shows good agreement with experiment at low Z,[19] but has not been tested for the Be I sequence at high Z.

The fine structures of the Cl XIV and Cl XV transitions are unresolved in our spectra and their use as calibration lines necessitates estimating their mean wavelengths. The transitions from the high-l states tend to dominate through both their large statistical weighting, and the relative transition probabilities for $\Delta n = 1$ transitions. We show in Fig. 3 the theoretical spectrum for the significant transitions in the Cl XV $n = 8$-9 complex, assuming initial statistical populations and hydrogenic transition probabilities. It should be noted that $\Delta L = -1$ transitions are predominant, the yrast line $8k$-$9l$ being the strongest, and also that the strongest components are separated by less than 0.1 Å. Superposed on the spectrum is the enve-

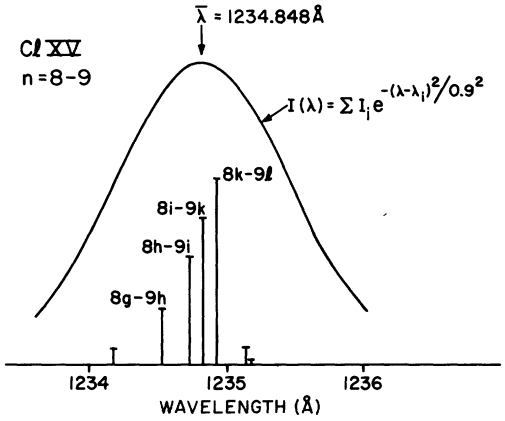

FIG. 3. The Cl XV $n=8$-9 complex. The envelope is the sum of the profiles with linewidths typical for the experiment, and is closely symmetric.

lope expected for linewidths typical for our experiment. The profile is slightly asymmetric, but this asymmetry is negligible at the signal-to-noise levels used in the experiment (see Figs. 1 and 2).

The centroid is determined as the calibration wavelength. This centroid wavelength is dependent on the initial relative populations of the $n=9$ states, which we have assumed to be statistical. Previous beam-foil measurements[21] on the Cl VII $n=6$-7 transitions near 2520 Å have shown statistical populations for the high-L transitions. Lennard and Cocke[22] have observed populations that increase more strongly with L than $(2L+1)$ for Fe^{n+} $(n=4$–$7)$. Hence we have also calculated the centroid wavelength of the $n=8$-9 complex for an L^2 population dependence and found that it differs by only 0.008 Å from that for a $(2L+1)$ dependence. An additional approximate verification of the $(2L+1)$ dependence is provided by the intensity ratios observed for the Cl XIV $5f$-$6g$ and $5g$-$6h$ transitions. As the mean lives and transition rates of the fine-structure components are different, their relative intensities change as a function of distance along the beam, with a consequent change in the mean wavelength. The change is +0.011 Å per cm for the $n=8$-9 transition in an 80-MeV chlorine beam. Our measurement was averaged over the first 5 mm of the decay. The estimated uncertainty in the centroid wavelength of the Cl XV $n=8$-9 transition from all the above contributions is ±0.010 Å, its value being 1234.50 Å.

The Cl XIV $n=8$-9 calibration wavelength is found similarly. The fine-structure separations are more than doubled, due to the nonzero core polarization. However, the line complex is still close to symmetric for the experimental signal-to-noise ratio. The centroid wavelength is then 1416.78 Å compared with 1418.56 Å neglecting the core polarization.

The core polarization has been treated only to first order and also nonrelativistically. A recent treatment by Dalgarno and Shorer[23] reproduces the splitting observed in the $n=5$-6 transitions of Cl XIV, but as noted above, these results are strongly affected by the mixing of the displaced term members. Assuming the same fractional perturbation of the $2s8l$ ionization potential as is observed from the mixing in the $2s6l$ levels leads to a wavelength shift in our observed transition of 25% of the total polarizability correction. Although the mixing is clearly less than this, we take this value of ±0.11 Å as the predominant source of error in this wavelength.

B. Wavelength separation

The wavelength dispersion in angstroms per pulse of the drive stepping motor was calculated from the known parameters of the mechanical system and was 0.069 44 in first order. This dispersion was checked over a large wavelength range (0 to 3130 Å) using a stationary mercury light source and a nonrefocused monochromator. The two numbers agreed to within 1 in 10^4. Since the separation to be measured is about 7.2 Å, this gives a precision of 10^{-3} Å. We have investigated in detail long scale nonlinearities of near-normal incidence monochromators in general and of the McPherson model 225 in particular. In this monochromator, small systematic variations in the dispersion occur due to the cam-driven motion of the grating and the refocusing procedure for fast-beam imaging, both of which cause a small change in the angle subtended by the slits at the grating center. Other small contributions to the dispersion error can be caused by (1) differential temperature expansion of the lever arm, the grating and the screw drive, (2) the degree of alignment of grating groves, (3) placement of the grating arm bearing on the grating normal, and (4) position and flatness of the optical flat which guides the grating arm bearing. These contributions are estimated to affect the dispersion at or below the 10^{-4} level and their combined effect can conservatively be estimated to give an error of less than one part in 10^3 which corresponds to an error of 5 mÅ in the $^3S_1$-$^3P_2$ wavelength.

The largest systematic error is expected from the positioning of the drive screw; eccentric placement of the bearings on the screw shaft can lead to a periodic error in the wavelength with a period corresponding to one revolution of the screw. This was tested with a stationary mercury light source by measuring variations in the wavelength

separations of six transitions in the range 2400–2700 Å, with a 600 l/mm grating, as their position on the screw is varied over 1.2 periods (60 Å). This was done by adjusting the grating to offset the zero-order reflection from −30 to 30 Å. The differential wavelength shifts were fitted to periodic functions to obtain a best fit. The resulting periodic amplitude yields a probable error of 15 mÅ in our wavelength separation measurement due to a periodic dispersion variation.

Significant Doppler shifts must be accounted for. Thus the observed wavelength λ_{obs} is given by

$$\lambda_{obs} = \lambda_0 \gamma (1 - \beta \cos\theta), \tag{6}$$

where λ_0 is the emitted wavelength, $\beta = v/c$ is the beam velocity ($\beta \approx 0.08$), $\gamma = (1-\beta^2)^{-1/2}$, and θ is the angle between the beam axis and the observation direction. The angle θ is close to 90° so that the first-order Doppler shift is small. We can estimate θ from measuring the spectrum as a function of beam energy. Some results are shown in Fig. 4. The second-order Doppler shift constitutes most of the observed shift, and a fit of Eq. (6) to the differential shifts of Fig. 4 yields a value of $\theta = 89.7 \pm 0.1°$. This angle difference of 0.3° from 90° changes our observed wavelength intervals by 0.003 Å and we assume an estimated precision of ±0.003 Å.

An additional check on the stability of the scanning monochromator can be obtained from these same spectra: The Lyman-α emission comes from excited hydrogen impurity atoms ejected at low velocity from the carbon foil. The wavelengths at different beam energies are found to be identical within the precision of these measurements.

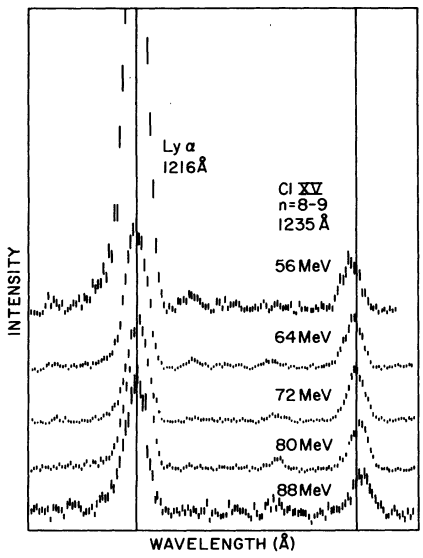

FIG. 4. Spectra of beam-foil excited chlorine at beam energies from 56 to 88 MeV showing principally the second-order Doppler shift which is linear in the energy.

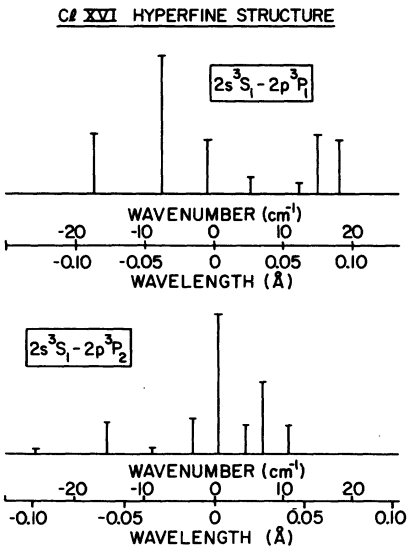

FIG. 5. The estimated hyperfine structures of the Cl XVI $2s\,^3S_1 - 2p\,^3P_{1,2}$ transitions.

The Cl XVI $2s$-$2p$ transitions contain hyperfine structure, but it is small and can be neglected for spectra with the linewidths obtained in these experiments. However, since future experiments are expected with considerably smaller linewidths (a few tenths of 1 Å) and better statistics, we reproduce in Fig. 5 the expected hyperfine structure for the $2s\,^3S_1$-$2p\,^3P_1$ and $2s\,^3S_1$-$2p\,^3P_2$ transitions of the ^{35}Cl isotope. The centroid of the hyperfine components is that of the transition without hyperfine structure.

All spectra have been fitted to sums of Gaussian profiles with the heights, widths, and centers as

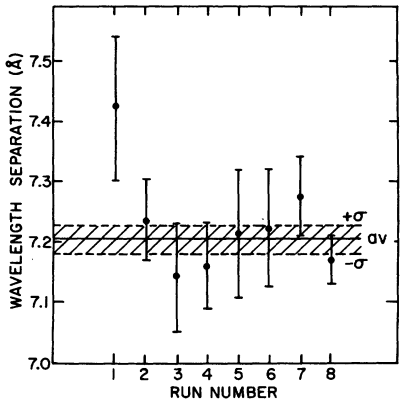

FIG. 6. The results of eight measurements of the wavelength interval from $2s\,^3S_1$-$2p\,^3P_2$ of Cl XVI and the calibration line n=8-9 of Cl XV.

TABLE I. Resumé of measurement errors (in m Å) for each transition $2s\,^3S_1$-$2p\,^3P_{0,2}$.

Upper level error	$^3P_2$	$^3P_0$
Population	8	8
Mean life	3	3
Profile asymmetry (hfs, etc.)	5	5
Dispersion (a) linear	1	1
Dispersion (b) periodic	15	15
Polarizability	1	110
Temperature variations	3	3
Grating alignment and similar mechanical errors	3	3
First- and second-order Doppler shifts	3	3
Statistics	12	100
Total error (rms)	22	150

parameters. The χ^2 sums showed that these profiles fit the data adequately, well within the statistics. In Fig. 6, we show the results of eight fits for the wavelength separation of the $2s\,^3S_1$-$2p\,^3P_2$ Cl XVI transition and the $n=8$-9 Cl XV calibration transition. The eight fits have a mean square deviation of $1\sigma=0.024$ Å about the weighted mean wavelength which agrees with the expected uncertainty from the error bars of the individual curves. The Cl XVI transition is observed in second order; this statistical error is halved to ±0.012 Å. We conclude that the major contribution to the final fitting uncertainty is the low statistics of each individual measurement. The systematic uncertainties discussed above, plus the uncertainties in the fit are summarized in Table I. The table also gives the total experimental error (1 s.d. confidence) in the wavelengths of the two $2s$-$2p$ transitions.

IV. TRANSITION ENERGIES OF THE TWO-ELECTRON SYSTEM

As discussed previously,[1] the term energies of a many-electron system can be written as sums of a nonrelativistic energy E_{NR}, based on the nonrelativistic Hamiltonian, plus relativistic energy corrections E_{REL}, plus quantum electrodynamic corrections E_{QED}. The latter two terms are generally treated perturbatively and separately. A question to be answered is where the approximate, and generally used, Breit Hamiltonian breaks down. Thus, in the two-electron system, the electron-electron interaction has been calculated to all orders nonrelativistically (the $1/r_{12}$ interaction), whereas two-photon exchange (and higher) terms are not calculated relativistically. Such a two-photon exchange, shown in Figs. 7(a) and 7(b) is formally of the same order as first-order screening of the one-electron Lamb shift terms. Such a lowest-order correction is also shown in Fig. 7(c). Some estimates of many-electron corrections to the one-electron Lamb shifts have been discussed by Ermolaev.[4] An interesting alternative approach to the relativistic many-electron atom has been given by Detrich.[24] The usual approach is through a Dirac-Hartree-Fock method as in the Desclaux program.[25]

The nonrelativistic parts of the energies for the $2s\,^3S$ and $2p\,^3P$ terms of the two-electron isoelectronic sequence have been calculated by Z-dependent variational perturbation theory (VP) with the result expressible in a power series in $1/Z$. Blanchard[26] concluded that the most accurate calculations for the $2s\,^3S$ state energy are those of Aashamar *et al.*,[27] while the results of Sanders and Scherr[28] should be taken for the $2p\,^3P$ state. For chlorine, $Z=17$, the $1/Z$ series rapidly converges to within 0.1 cm^{-1} with five terms of the series. The value given in Table II for the nonrelativistic transition energy agrees with a recent calculation of Ermolaev[29] to within 0.1 cm^{-1}. The mass polarization correction is taken from Ermolaev and Jones[29] for the $2p\,^3P$ state. This correction for the $2s\,^3S$ state is given by Accad *et al.*[30] up to $Z=10$ and we have used extrapolated values for higher Z where it is very small (0.6 cm^{-1}).

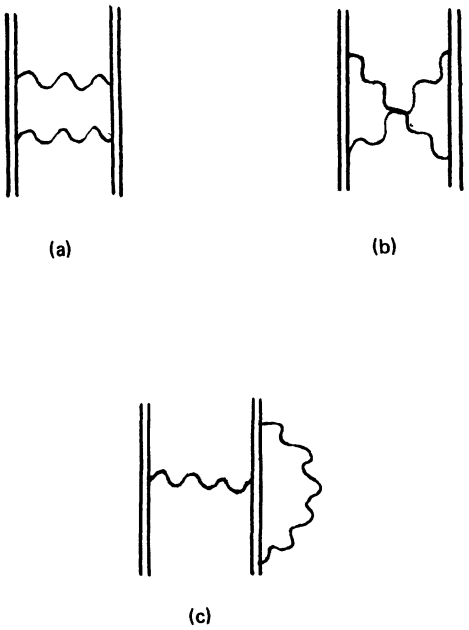

FIG. 7. Two-photon diagrams which have not been included in the theory.

TABLE II. Transition energy of $2s$-$2p$ in Cl XVI (cm^{-1}).

	$2s\,^3S_1$-$2p\,^3P_2$	$2s\,^3S_1$-$2p\,^3P_0$
Nonrelativistic ΣZ^{-n}	135 256.3	135 256.3
Mass polarization	−70.0	−70.0
Relativistic		
1-e Dirac fine structure	30 800.2	0.0
Breit+photon exch $Z(\alpha Z)^2$	−2 084.0	8 201.1
Extrap. Breit $(\alpha Z)^2(1+1/Z+\cdots)$	−2.3	−873.6
+photon exch $Z[(\alpha Z)^4+\cdots]$	−27.0	90.9
Total (rel.+nonrel.)	163 873.2	142 604.7
	(610.228 Å)	(701.239 Å)
QED terms		
$S_{SE}^{(2)}$ $(1/\alpha)(\alpha Z)^4\Sigma(\alpha Z)^n$	−1 040.7	−1 106.9
$S_{VP}^{(2)}$ $(1/\alpha)(\alpha Z)^4\Sigma(\alpha Z)^n$	69.2	69.2
$S_{SE}^{(4)}$ $(\alpha Z)^4$	−0.28	−0.28
S_{RM} $(1/\alpha)(\alpha Z)^4 m/M$	0.03	0.03
S_{RR} $(1/\alpha)(\alpha Z)^5 Zm/M$	−0.71	−0.71
S_{NS} $(1/\alpha^2)[(\alpha Z)^4+(\alpha Z)^6]$	−6.93	−6.93
Total QED	−979.4	−1 045.6
Total transition energy		
Rel.+nonrel.+QED	162 893.8	141 559.1
	(613.897 Å)	(706.419 Å)

The relativistic energy terms can be included formally within a double expansion in $\lambda = 1/Z$ and $\mu = \alpha^2 Z^2$, where α is the fine-structure constant. Calculations which are not based on the $1/Z$ expansion can still be expressed approximately as part of the double series by considering the order of perturbation theory used. Ermolaev and Jones[31] have compared in detail the Z-expansion calculations of Layzer and Bahcall[32] with the relativistic Hartree-Fock equations and the Breit-Pauli methods. We can write the term energies in atomic units as

$$E = Z^2 \sum_{p,q=0}^{\infty} \epsilon_{pq} \lambda^p \mu^q , \tag{7}$$

where the expansion parameters ϵ_{pq} which have to be calculated, form a square doubly infinite matrix. The first column of parameters, $\sum_{i=0}^{\infty} \epsilon_{i0}$, consists of the nonrelativistic $1/Z$ expansion, while the first row, $\sum_{i=0}^{\infty} \epsilon_{0i}$, corresponds to the sum of the one-electron Dirac energies of an atom of nuclear charge Z expressed as a series expansion in $\alpha^2 Z^2$. Thus, the first relativistic term given in Table II is the sum of terms $\epsilon_{0j}\mu^j$ for $j = 1, \infty$. The first-order correction ϵ_{11} of the one-electron relativistic energy due to the Breit interaction has been calculated by Doyle.[33] The remaining terms of the second row of Table III, $\epsilon_{1j}(j > 1)$, consist of the first-order correction of the Breit interaction to the relativistic wave function and energy, calculated by Mohr[7] for the $2p\,^3P_0$ term and by Cheng[34] for the $2p\,^3P_2$ term. The remaining terms of the second column of Table III, $\epsilon_{i1}(i > 1)$, consist of the first-order correction of the Breit interaction, in the Pauli approximation,

TABLE III. Double expansion of an atomic energy E in terms of $\lambda = 1/Z$ and $\mu = \alpha^2 Z^2$ [Eq. (7)].

	μ^0	μ^1	μ^2
λ^0	ϵ_{00}	ϵ_{01}	$\epsilon_{02}\rightarrow$ Dirac fine structure
λ^1	ϵ_{10}	Doyle	Mohr + Cheng →
λ^2	ϵ_{20}	Pekeris ext	$\epsilon_{22}\cdots$
	↓	↓	.
	Nonrelativistic $1/Z$ expansion		.

to the nonrelativistic variational wave function and energy. Mohr[7] has estimated the sum of these corrections for $Z=18$ from the results of Accad *et al.*[30] who calculated the terms explicitly for $2<Z\leq 10$. Following the same scheme, we have generated estimates for higher Z using the dominant Z dependence of the correction. These estimates vary from those of Mohr by a few wave numbers for $Z=18$. The Doyle-term energy correction ϵ_{11} and the energy corrections from the remainder of the second column $\epsilon_{i1}(i>1)$ and the second row $\epsilon_{1j}(j>1)$ are listed separately in Table II.

The next higher-order expansion parameter ϵ_{22} in the third row and column of Table III has not been calculated and includes higher-order relativistic corrections; e.g., the relativistic two-photon exchange terms of Fig. s 7(a) and 7(b). To the authors' knowledge, calculations have been made of this term (and some higher-order corrections), only for the fine structure in He I (see Ref. 35). The calculation for the fine structure of the ^3P states of He I have generally been expressed as a series expansion of α up to α^6 terms and hence some of the terms included in Table II have not been included there. It is clear from the magnitudes of the series terms that the uncalculated corrections are higher for the $^3P_0$ state than for the $^3P_2$ state. These magnitudes suggest the energy corrections due to ϵ_{22} and higher terms should be of the order of 10 cm^{-1} for $^3P_2$ and about 100 cm^{-1} for the $^3P_0$ terms for chlorine.

The quantum-electrodynamic terms in Table II are taken directly from the one-electron calculations which have been summarized by Mohr[36] for the $^3P_0$ term ($2p_{1/2}$). The j-dependent corrections necessary for the $^3P_2$ term ($2p_{3/2}$) have been taken from Garcia and Mack's[37] formulation of the results of Erickson and Yennie.[38] The corrections occur only in the first few terms of the self-energy expression $S_{SE}^{(2)}$ and are due to the electron's anomalous magnetic moment. We note that no estimate of the effect of the second electron on the Lamb shift is included. For example, we have neglected diagrams of the type shown in Fig. 7(b).

For completeness, in Table IV we present the results of the Z-expansion calculations for the transition wave numbers of $2s\,^3S_1$-$2p\,^3P_{0,2}$ for nuclear charge $Z=2$–22 and compare them with experiment. The results at low Z are naturally close to those of Accad *et al.*,[30] since we have used their relativistic corrections as part of an $\alpha^2Z^4\Sigma(1/Z)^n$ expansion and since the other relativistic terms are very small (less than 1 cm^{-1}) for these Z values. At higher Z up to $Z=17$, the theoretical value for the transition from $^3P_2$ is approximately 10 cm^{-1} lower than experiment,

TABLE IV. He I isoelectronic sequence $2s\,^3S_1$-$2p\,^3P_{02}$ transition. (The value in parentheses indicates the precision in the last numbers.)

Z	$2s\,^3S_1$-$2p\,^3P_2$ Expt.	$2s\,^3S_1$-$2p\,^3P_2$ This calc.	$2s\,^3S_1$-$2p\,^3P_0$ Expt.	$2s\,^3S_1$-$2p\,^3P_0$ This calc.
2	9230.823	9231.37	9231.002	9232.58
3	18227.044	18227.24	18230.150	18230.30
4	26867.9(2)	26966.1	26865(2)	26863.1
5	35429(1)	35427.2	35393(1)	35390.6
6	44022(1)	44018.1	43899(1)	43894.0
7	52720(6)	52714.7	52416(1)	52413.2
8	61595(1)	61582.0	60983(3)	60968.4
9	70700(3)	70691	69586(3)	69576.8
10	80121(1)	80111	78267(2)	78252
11		89931	78267(2)	86993
12		10237		96141
13		111133		104746
14	122775(60)	122721	113856(90)	113771
15		134956		122911
16		148470		132169
17	162913(6)	162893	141707(30)	141558
18	178508(300)	178545	151355(250)	151091
19		195566		160761
20		214138		170589
21		234436		180586
22		256644		190754

e.g., for $Z=8$, 9, 10, and 17. Less accurate measurements for $Z=14$ by O'Brien *et al.*[9] also suggest the same trend. As expected from the larger magnitude of the relativistic corrections of the transition from $^3P_0$, comparisons with experiment show discrepancies of the order of 100 cm^{-1} for $Z=17$ and perhaps for $Z=14$. The accuracies of these measurements, however, are not really sufficient to test the theory. Further precision measurements are needed to test the reliability of the relativistic Z-expansion results.

However, it is clear that the present experimental results in Cl XVI test the combined relativistic and quantum electrodynamic corrections to less than 1% of the QED part. This is considerably more accurate than the recent measurement of the QED Lamb shift in hydrogenic argon by Gould and Marrus.[8] It is noteworthy to compare the quantum-electrodynamic correction derived from our result for the $^3S_1$-$^3P_2$ transition in Cl XVI, assuming the relativistic and nonrelativistic contributions are correct with the two theoretical results of Mohr[36] and Erickson.[39] These two calculations differ only in their results for the self-energy term (denoted by $S_{SE}^{(2)}$ in Table II). In Fig. 8, we have scaled the theoretical results to give constant differences for $Z=1$, 17, and 18. At high Z, the QED calculations of Cheng and Johnson[40] show agreement with those of Mohr. At

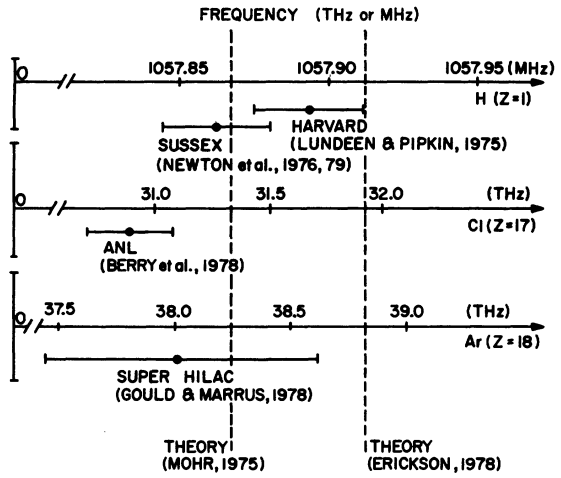

FIG. 8. Comparisons of experimental Lamb-shift precision with the theories of Mohr and Erickson for $Z=1$–18. The references are given in the text.

$Z \approx 137$ the point nucleus calculations of Cheng and Johnson, Labzovskii,[41] and of Mohr show a singularity as expected, while the results of Erickson do not (as seen in Fig. 2 of Ref. 40). From these considerations, the Mohr QED calculations should be the most reliable for $Z \gtrsim 10$. The precision of the two theories below $Z=10$ may be comparable because of extrapolations made in the work of Mohr. It is clear from Fig. 8 that recent experiments[42,1,8] show better agreement with Mohr, our two-electron result being slightly low, most probably due to uncertainty in the relativistic corrections of about 10 cm^{-1}.

V. TRANSITION ENERGIES OF THE THREE-ELECTRON SYSTEM

In this section, we present two different calculations of the energies of the resonance transitions $2s\,^2S_{1/2}$-$2p\,^2P_{1/2,3/2}$ of the Li I isoelectronic sequence, and compare the results with existing experiments. Since the resonance transitions are more easily produced in most spectral light sources, far more measurements exist for these $2s$-$2p$ transitions than for the two-electron ions. Hence, the increased difficulty of the theory is balanced by this more comprehensive comparison with experimental data. It is to be hoped that the Z dependence of the discrepancies between theory and experiment can indicate where the theory is inadequate. In particular, it is desirable to distinguish between uncalculated electron correlations and screening corrections to the quantum-electrodynamic terms. Eldén[18] has recently published a parametric fit of existing data for these two transitions, so that wavelengths can be predicted very accurately for higher-Z ions in this sequence. Our results are generally in good agreement with Edlén's predictions.

Cheng[34] has applied the relativistic Hartree-Fock program of Desclaux[25] to derive the transition energies of the $2s_{1/2}$-$2p_{1/2,3/2}$ transitions. To these energies, we have added the quantum-electrodynamic corrections as defined by Mohr[36] for the $p_{1/2}$ electron, together with the j-dependent corrections which have been listed by Erickson[38] and by Garcia and Mack,[37] with no screening included. The results are listed in Tables V and VI as E_{DF} (cm^{-1}) for nuclear charge $Z=3$–40.

In an alternative energy calculation, we have followed our procedure for the two-electron system in writing the energy as a series of terms:

$$E = E_{NR} + E_{REL} + E_{QED} + E_{M}\,, \tag{8}$$

where the terms on the right of Eq. (8) represent, respectively, the nonrelativistic energy, the relativistic energy, the quantum-electrodynamic energy, and the mass polarization correction.

In the expansion of the nonrelativistic energy as a $1/Z$ sequence, only the first few terms are known accurately. From the results of earlier work of Horak *et al.*[43] and Seung and Wilson,[44] for example, Ivanova and Safronova[45] give the following expressions for variational energies of the ^2S and ^2P terms (in a.u.):

$$E_V(^2S) = -1.125Z^2 + 1.022\,81Z - 0.408\,2\,, \tag{9}$$

$$E_V(^2P) = -1.125Z^2 + 1.093\,53Z - 0.528\,6\,. \tag{10}$$

They also obtain the Hartree-Fock (HF) energies:

$$E_{HF}(^2S) = -1.125Z^2 + 1.022\,81Z - 0.354\,549 - 0.041\,35/Z\,, \tag{11}$$

$$E_{HF}(^2P) = -1.125Z^2 + 1.093\,53Z - 0.469\,462 - 0.107\,58/Z\,. \tag{12}$$

The variational and Hartree-Fock energies differ in the third term due to neglect of some electron correlation in the Hartree-Fock calculation. Clearly this leads to a constant energy difference between the real and Hartree-Fock energies, plus higher-order corrections proportional to $1/Z$, $1/Z^2$, etc., which will become small for higher members of the isoelectronic sequence. We obtain two nonrelativistic ^2S-^2P transition energies from Eqs. (9)–(12):

$$E_{NR}^{VAR} = 0.070\,72Z - 0.120\,4 - 0.066\,23/Z\,, \tag{13}$$

$$E_{NR}^{HF} = 0.070\,72Z - 0.114\,913 - 0.066\,23/Z\,. \tag{14}$$

The two results differ by the constant 0.0055 a.u. (1207 cm^{-1}). Note that we have added the HF $1/Z$ term to the "variational" energy in Eq. (13) since this term has not been previously estimated vari-

TABLE V. Li I isoelectronic sequence $2s_{1/2}$-$2p_{1/2}$ transition.

Z	$E_{expt}(cm^{-1})$	$E_{DF}(cm^{-1})$	$E_{VS}(cm^{-1})$	$E_E(cm^{-1})$	$E_{QED}(cm^{-1})$
3	14 903.7	14 850	15 298	14 903.7	−2.1
4	31 928.8	32 172	32 049	31 928.7	−6.0
5	48 358.5	48 822	48 335	48 358.4	−13.5
6	64 483.9	65 095	64 404	64 483.8	−26.1
7	80 463.2	81 173	80 364	80 463.2	−45.4
8	96 375	97 154	96 273	96 374.5	−73.2
9	112 260.4	113 091	112 167	112 262	−111.5
10	128 151.9	129 017	128 068	128 152	−162.0
11	144 057(8)	144 956	143 992	144 064	−227
12	160 015(5)	160 924	159 953	160 012	−309
13	176 009(8)	176 934	175 964	176 009	−409
14	192 042(7)	192 996	192 031	192 063	−531
15	208 151(17)	209 120	208 164	208 183	−675
16	224 361(10)	225 315	224 373	224 377	−846
17	240 674(23)	241 586	240 654	240 654	−1 045
18	256 997(13)	257 945	257 030	257 020	−1 276
19		274 397	273 498	273 481	−1 539
20	290 023(25)	290 948	290 068	290 046	−1 838
21		307 604	306 747	306 722	−2 176
22	323 468(90)	324 373	323 539	323 516	−2 556
23		341 262	340 454	340 434	−2 980
24	357 359(25)	358 277	357 494	357 486	−3 451
25	374 700(28)	375 424	374 670	374 678	−3 973
26	392 003(31)	392 712	391 988	392 019	−4 546
27		410 144	409 453	409 517	−5 177
28	426 985(36)	427 734	427 076	427 182	−5 864
29		445 470	444 854		−6 621
30		463 383	462 806		−7 438
31		481 463	480 930		−8 329
32		499 726	499 239		−7 290
33		518 178	517 741		−10 327
34		536 818	536 437		−11 447
35		555 670	555 344		−12 647
36	574 380(1×10^3)	574 720	574 460		−13 941
37		593 997	593 804		−15 319
38		613 493	613 374		−16 799
39		633 232	633 193		−18 371
40		653 202	653 250		−20 054
45		756 921	758 772		−30 226

ationally. A comparison of the Hartree-Fock expansion with the precision Hartree-Fock calculations of Weiss[46] for $2s$-$2p$ of $Z=3$–10 gives a value for the next term in the expansion (14) of $-0.075/Z^2$. (This is not included in our tables.)

We estimate the relativistic energy of the three-electron system in a generalization of the Dirac energy for a one-electron atom: Thus, for each term (in a.u.):

$$E_R=\sum_i [E^{(i)}_{\text{Dirac}}(Z_i)+Z_i^2/2n_i^2]. \tag{15}$$

Equation (15) represents the sum of screened Dirac energies $E^{(i)}_{\text{Dirac}}(Z_i)$ with the nonrelativistic term $Z_i^2/2n_i^2$, removed for each electron i in the atom. Thus each i represents the electrons $1s$ and $2s$ or $2p_{1/2}$ or $2p_{3/2}$. $E^{(i)}_{\text{Dirac}}(Z_i)$ represents the regular Dirac energy (excluding the mass term) in a Coulomb field of screened nuclear charge $Z_i=Z-\sigma_i$.

This formulation is identical to what has been used above for the two-electron system, save for the introduction of the screening constants σ_i, i.e., no screening was used in the two-electron system. The screening constants introduce the many-electron corrections to the relativistic energy which were calculated explicitly for the two-electron systems, at least for the first few terms of the α^2Z^2 expansion, as in the first-order Breit interaction. The mutual screening of each pair of electrons can be evaluated within the two-electron system as a contribution to the Breit interaction.

TABLE VI. Li I isoelectronic sequence $2s_{1/2}$-$2p_{3/2}$ transition.

Z	$E_{expt}(cm^{-1})$	$E_{DF}(cm^{-1})$	$E_{VS}(cm^{-1})$	$E_E(cm^{-1})$	$E_{QED}(cm^{-1})$
3	14 904	14 850	15 297	14 904.0	−2.0
4	31 935.4	32 177	32 054	31 935.3	−5.8
5	48 392.6	48 853	48 368	48 392.5	−13.0
6	64 591.8	65 198	64 510	64 591.1	−25.1
7	80 721.7	81 437	80 623	80 722.2	−43.4
8	96 907.5	97 677	96 806	96 905.9	−69.8
9	113 236.2	114 056	113 146	113 237	−106.2
10	129 801.2	130 654	129 725	129 802	−153.8
11	146 688(8)	147 565	146 628	146 690	−215
12	163 991(5)	164 882	163 946	163 992	−292
13	181 802(7)	182 707	181 779	181 807	−386
14	200 228(8)	201 146	200 230	200 241	−499
15	219 409(14)	220 313	219 415	219 409	−634
16	239 423(11)	240 333	239 454	239 434	−794
17	260 444(27)	261 339	260 482	260 448	−979
18	282 582(16)	283 472	282 640	282 593	−1 192
19		306 884	306 077	306 019	−1 436
20	330 907(34)	331 737	330 955	330 890	−1 713
21		358 201	357 446	357 376	−2 025
22	385 743(45)	386 457	385 728	385 659	−2 375
23		416 700	415 996	415 933	−2 765
24	448 430(40)	449 131	448 450	448 400	−3 198
25	483 325(46)	483 961	483 303	483 276	−3 678
26	520 725(54)	521 423	520 783	520 786	−4 203
27		561 704	561 121	561 169	−4 782
28	604 522(180)	605 183	604 571	604 676	−5 410
29		651 980	651 378		−6 105
30		702 431	701 831		−6 852
31		756 804	756 203		−7 666
32		815 408	814 796		−8 543
33		878 522	877 921		−9 489
34		946 553	945 897		−10 510
35		1 019 766	1 019 069		−11 603
36	1 097 695(2×10^3)	1 098 523	1 097 779		−12 781
37		1 183 215	1 182 407		−14 035
38		1 274 207	1 273 322		−15 382
39		1 371 917	1 370 936		−16 811
40		1 476 739	1 475 648		−18 341
45		2 123 381	2 122 644		−27 588

Thus, the total screening of one electron by the other electrons in the atom is derived from the two-electron system. Snyder[47,48] has used this comparison to obtain the first-order values of the screening constants σ_i.

The approximation can be expected to break down at higher Z, where the two-electron Breit approximation to the relativistic Hamiltonian will also break down. In addition, the nonrelativistic energy as the second term of Eq. (15) should be inadequate especially at low Z where $1/Z$, $1/Z^2$, etc., terms are neglected. This effect can be seen as an undershoot in the theory for low Z, as is observed in Figs. 9–11. We have included in Figs. 10 and 11 the comparisons for both nonrelativistic approximations of Eqs. (13) and (14) to show that the Hartree-Fock result differs from experiment by only the Z-independent electron correlation term.

However, this model suffers the general drawback of all Z-expansion calculations that at high Z, it must break down. In addition, evaluation of the screening constants necessary for $n=3$ and higher shells is not straightforward although high-order relativistic and QED effects become very small. Also, the distinction between relativistic corrections included in this model and higher-order quantum-electrodynamic corrections is not clear *a priori*. The same problem exists also for the present relativistic Hartree-Fock formulation of Desclaux, as used in this paper.

The quantum-electrodynamic term E_{QED} of Eq.

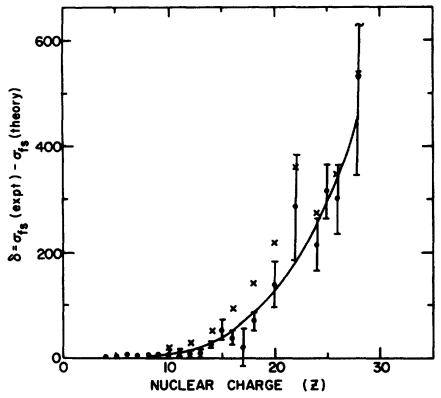

FIG. 9. The fine structure of the $2p\,^2P$ state of the Li I isoelectronic sequence. The difference of experiment and the relativistic splitting (the crosses from Dirac-Fock calculations, the filled circles from Snyder screening, with error bars from experiments; the same error bars have been omitted from the crosses for clarity) is plotted as a function of nuclear charge Z. The curve represents the QED correction for hydrogenic $2p_{1/2}$-$2p_{3/2}$ electrons.

(8) is taken as the one-electron Lamb shift for the $2p_{1/2}$ and $2p_{3/2}$ electrons without any shielding. The mass polarization term E_M of Eq. (8) has been evaluated by Hughes and Eckart[49] and is small for

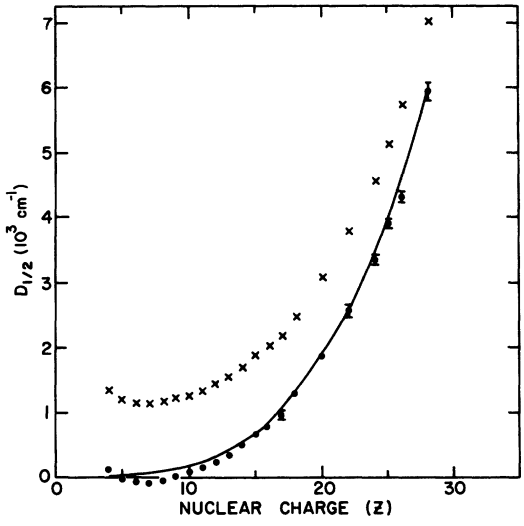

FIG. 10. The wave number of the $2s\,^2S_{1/2}$-$2p\,^2P_{1/2}$ transition. The difference of experiment and calculations omitting all QED corrections is plotted against nuclear charge Z. The crosses represent Hartree-Fock $1/Z$ nonrelativistic plus the screened relativistic calculations. For the filled circles, the HF calculation is replaced by variational $1/Z$ nonrelativistic theory. The curve represents the QED correction (i.e., Lamb shift). for the hydrogenic $2s_{1/2}$-$2p_{1/2}$ electrons. The error bars are taken from the experiments.

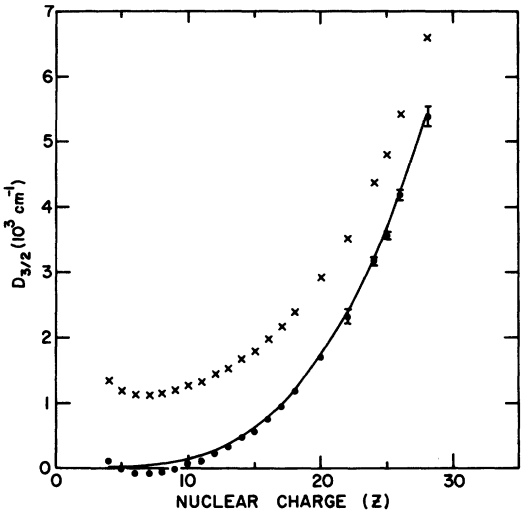

FIG. 11. The wave number of the $2s\,^2S_{1/2}$-$2p\,^2P_{3/2}$ transition. The symbols are the same for $D_{3/2}$ as for $D_{1/2}$ in Fig. 10.

all Z. Adding together the results of the calculations for all four terms on the right-hand side of Eq. (8), we now obtain the transition energies for the $2s$-$2p_{1/2}$ and $2s$-$2p_{3/2}$ transitions of the lithium-like ions. These energies are listed in Tables V and VI for $3 \leq Z \leq 40$. The results using the nonrelativistic Eq. (13) are listed as E_{VS} and the semiempirical calculations of Edlén[18] (E) are listed as E_E. The experimental results are taken from the same sources listed by Edlén,[18] plus some recent data on Ti, Cr, Fe, Ni, and Kr.[50] In comparing experiment and theory, we note that apart from $Z=3$ and 4, the variational screening (VS) calculation E_{VS} agrees more closely with experiment than the Dirac-Fock energy E_{DF}, and for $Z>13$, E_{VS} agrees with experiment within experimental error (except for $Z=24$).

A principal result of these comparisons is that the *unscreened* one-electron Lamb shift should be used to obtain agreement between experiment and theory. In particular, the fine structure, which is independent of the nonrelativistic model used, shows that the quantum-electrodynamic part is unscreened. In Fig. 9 we show the difference between the experimental fine structure and the non-QED relativistic calculations for $Z \leq 40$. This difference is well fitted by the unscreened Lamb shift for both the Dirac-Fock and the screened relativistic model. In Figs. 10 and 11 we compare the differences of the experimental transition energies and the non-QED calculations to show that the unscreened Lamb shifts provide very good fits to the data. The experimental precision at high Z is sufficient to provide very accurate tests of QED and the relativistic corrections. For example,

TABLE VII. The $2s$-$2p$ transitions in Cl XVI.

Transition	Observed wavelength (Å)	Observed wave number (cm^{-1})	Calculated wave number (cm^{-1})
$^3S_1$-$^3P_2$	613.825 ± 0.022	162 913(6)	162 893(10)
$^3S_1$-$^3P_0$	705.68 ± 0.150	141 707(30)	141 558(100)

for $Z=24$, 25, 26, and 28, the experimental precision is between 0.6 and 0.8% of the Lamb shift.

VI. CONCLUSIONS

This more detailed analysis of possible systematic errors in our measurements[1] of the $2s$-$2p$ transitions in Cl XVI has resulted in a small change in our values for the wavelengths and wave numbers and a small increase in the total estimated experimental error. Also, further analyses of the relativistic contributions to the $2s$-$2p$ transition have produced some small changes to those previously published.[1] The results are shown in Table VII. The quoted theoretical error is based only on possible errors due to higher-order relativistic corrections, the total of which are assumed to be of the same order as the previously calculated term. The size of the next order correction to the quantum-electrodynamic terms, due to an exchange of one photon between the two electrons during the emission of a virtual photon [Fig. 7(c)], is uncertain, but may be of the size of the present discrepancy (20 cm^{-1}) between experiment and theory for the $2s\,^3S_1$-$2p\,^3P_2$ transition. The experimental error limit represents one standard deviation of the sum of statistical and systematic errors. The two major sources of uncertainty are (a) statistical errors due to the small number of photons counted, and (b) a possible systematic error due to a periodic variation in the wavelength dispersion of the scanning monochromator. A further source of error for the $^3P_0$ measurement is the lack of a well-known polarizability for the Cl XIV $n=8$–9 calibration line. Clearly, these three major sources of error can be reduced.

We conclude that in these high-Z ions, we can make tests of quantum electrodynamics which are at least as accurate as those presently possible for one-electron systems. However, our results show that clear-cut tests of quantum electrodynamics at a precision of a few parts per thousand are limited by our present knowledge and formulation of relativistic quantum mechanics. Hence, the major value of precision wavelength measurements in high Z, few-electron ions, must be in stimulating a more consistent relativistic theory of many electron atoms beyond the present perturbation approaches using the Bethe-Salpeter equation.

As a corollary to these ideas we have included here a comparison of theory and experiment for the same $2s$-$2p$ transition in three-electron ions. For such systems, the Dirac-Hartree-Fock approach has provided the most precise calculations over the complete isoelectronic sequence. However, the incomplete treatment of electron correlations with this approach makes it much less accurate than most of the experimental measurements. We present, without any proof of its validity, an extension of Snyder's attempt to include nonrelativistic electron correlation with a screened relativistic calculation. Both the Dirac-Hartree-Fock and the screened relativistic calculations show precisions of a few hundred wave numbers up to as high a nuclear charge as has been measured. It is important to note that in these calculations, only the first-order, one-electron, unscreened quantum-electrodynamic terms have been included. These results suggest that the higher-order QED corrections may be much smaller than expected. As a consequence, precision measurements in other few-electron systems (including the two-electron case) may provide much cleaner tests of relativistic quantum mechanics and QED. Both the Dirac-Hartree-Fock and screened relativistic calculations can easily be extended to ions of 4–10 electrons with similar precision. This will allow a large amount of spectroscopic data to be compared directly with *ab initio* theory.

Note added. Since submission of this paper, two new sets of results have been published on the $2s\,^3S_1$-$2p\,^3P_{0,2}$ transitions, the first by Armour *et al.*, Phys. Lett. *75A*, 45 (1979) in Si XIII and the second by Livingston *et al.*, J. Phys. B 13, L139 (1980 on Si XIII, S XV, and Cl XVI. All the results have a precision of ±0.1 Å in wavelength and show agreement with the theoretical values of Table IV.

ACKNOWLEDGMENTS

We thank Kwok-tsang Cheng for his Dirac-Hartree-Fock calculations and innumerable helpful discussions. We also acknowledge with thanks Robert Brooks, Murray Peshkin, and Yong-Ki Kim at Argonne and Walter Johnson at the University of Notre Dame for their help and interest in this work. This research was performed under the auspices of the Department of Energy, Division of Basic Energy Sciences.

*This paper submitted in partial fulfillment for the requirements of the Ph.D. degree from the University of Chicago.

†Present address: University of Notre Dame, Notre Dame, Ind. 46556.

[1]H. G. Berry, R. DeSerio, and A. E. Livingston, Phys. Rev. Lett. 41, 1652 (1978).
[2]H. G. Berry and R. Bacis, Phys. Rev. A 8, 36 (1973).
[3]H. G. Berry and R. M. Schectman, Phys. Rev. A 9, 2345 (1974).
[4]A. M. Ermolaev, Phys. Rev. Lett. 23, 380 (1975); and work referenced therein.
[5]S. O. Kastner, Phys. Rev. A 6, 570 (1972).
[6]W. A. Davis and R. Marrus, Phys. Rev. A 15, 1963 (1977).
[7]P. Mohr, quoted in Ref. 6.
[8]H. Gould and R. Marrus, Phys. Rev. Lett. 41, 1457 (1978).
[9]R. O'Brien, J. D. Silver, N. A. Jelley, S. Bashkin, E. Träbert, and P. H. Heckmann, J. Phys. B 12, L41 (1979).
[10]J. A. Leavitt, J. W. Robson, and J. O. Stoner, Nucl. Instrum. Methods 110, 423 (1973).
[11]M. Dufay, A. Denis, and J. Desesquelles, Nucl. Instrum. Methods 90, 85 (1970).
[12]H. G. Berry and C. H. Batson, in *Beam-Foil Spectroscopy*, edited by I. A. Sellin and D. J. Pegg (Plenum, New York, 1975), Vol. 1, p. 367.
[13]W. N. Lennard and C. L. Cocke, Nucl. Instrum. Methods 110, 137 (1973).
[14]B. Edlén, in *Handbuch der Phvsik*, edited by S. Flügge (Springer, Berlin, 1964), Vol. 27.
[15]A. Dalgarno, Adv. Phys. 11, 281 (1962).
[16]A. Dalgarno and A. L. Stewart, Proc. R. Soc. London Ser. A 247, 245 (1958).
[17]L. Pauling, Proc. R. Soc. London Ser. A 114, 181 (1927); and see discussion in Ref. 15.
[18]B. Edlén, Phys. Scr. 19, 255 (1979).
[19]L. J. Curtis, Phys. Scr. 21, 162 (1980); and private communication.
[20]R. Hallin, Ark. Fys. 32, 201 (1966).
[21]Reference 4; and see E. Veje, Phys. Rev. A 14, 2077 (1976); and earlier publications listed therein.
[22]W. N. Lennard and C. L. Cocke, Nucl. Instrum. Methods 110, 137 (1973).
[23]A. Dalgarno and P. Shorer (private communication); and Phys. Rev. A 20, 1307 (1979).
[24]J. Detrich, Phys. Rev. A 5, 2014 (1972).
[25]J. P. Desclaux, Comput. Phys. Commun. 9, 31 (1975).
[26]P. Blanchard, Phys. Rev. A 13, 1698 (1976).
[27]K. Aashamar, J. Chem. Phys. 60, 3404 (1974).
[28]F. C. Sanders and C. W. Scherr, Phys. Rev. 181, 84 (1969).
[29]A. M. Ermolaev (private communication); and A. M. Ermolaev and M. Jones, J. Phys. B 7, 199 (1974).
[30]Y. Accad, C. L. Pekeris, and B. Schiff, Phys. Rev. A 4, 516 (1971).
[31]A. M. Ermolaev and M. Jones, J. Phys. B 6, 1 (1973).
[32]D. Layzer and J. Bahcall, Ann. Phys. (N.Y.) 17, 177 (1962).
[33]H. T. Doyle, in *Adv. in Atomic and Mol. Phys.*, edited by D. R. Bates and I. Estermann (Academic, New York, 1969), Vol. 5, p. 337.
[34]K. T. Cheng (private communication); also Y.-K. Kim and J. P. Desclaux, Phys. Rev. Lett. 36, 139 (1976).
[35]See, e.g., L. Hambro, Phys. Rev. A 5, 2027 (1972).
[36]P. J. Mohr, Phys. Rev. Lett. 34, 1050 (1975); and in *Beam-Foil Spectroscopy*, edited by I. A. Sellin and D. J. Pegg (Plenum, New York, 1976), p. 89.
[37]J. D. Garcia and J. E. Mack, J. Opt. Soc. Am. 55, 654 (1965).
[38]G. W. Erickson and D. R. Yennie, Ann. Phys. (N.Y.) 35, 271 (1965).
[39]G. W. Erickson, J. Phys. Chem. Ref. Data 6, 831 (1977).
[40]K. T. Cheng and W. Johnson, Phys. Rev. A 14, 1943 (1976).
[41]L. N. Labzovskii, Zh. Eksp. Teor. Fiz. 59, 2165 (1970) [Sov. Phys.–JETP 32, 1171 (1971)].
[42]The measurements in hydrogen are by S. Lundeen and F. M. Pipkin, Phys. Rev. Lett. 34, 1368 (1975); D. A. Andrews and G. Newton, *ibid.* 37, 1254 (1976); and G. Newton, D. A. Andrews, and P. J. Unsworth, Philos. Trans. R. Soc. London 290, 373 (1979).
[43]L. J. Horak, M. N. Lewis, A. Dalgarno, and P. Blanchard, Phys. Rev. 185, 21 (1969).
[44]S. Seung and E. B. Wilson, J. Chem. Phys. 47, 5343 (1967).
[45]E. P. Ivanova and U. I. Safronova, J. Phys. B 10, 1591 (1975).
[46]A. Weiss, Astrophys. J. 138, 1262 (1963).
[47]R. Snyder, J. Phys. B 4, 1150 (1971).
[48]R. Snyder, J. Phys. B 7, 335 (1974).
[49]D. S. Hughes and C. Eckart, Phys. Rev. 36, 694 (1930).
[50]E. Hinnov, Astrophys. J. 230, L197 (1979).